ISSN 1064-2307, Journal of Computer and Systems Sciences International, 2023, Vol. 62, No. 5, pp. 800–816. © Pleiades Publishing, Ltd., 2023.
ISSN 1064-2307, Journal of Computer and Systems Sciences International, 2023. © Pleiades Publishing, Ltd., 2023.
Russian Text © The Author(s), 2023, published in Izvestiya Akademii Nauk, Teoriya i Sistemy Upravleniya, 2023, No. 6, pp. 93–109.

SYSTEMS WITH DISTRIBUTED PARAMETERS

Optimization of Longitudinal Motions of an Elastic Rod Using Periodically Distributed Piezoelectric Forces

A. A. Gavrikov[a] and G. V. Kostin[a,*]

[a] *Ishlinsky Institute for Problems in Mechanics RAS (IPMech RAS), Moscow, 119526 Russia*

** e-mail: kostin@ipmnet.ru*

Received March 30, 2023; revised April 25, 2023; accepted June 5, 2023

Abstract—The longitudinal vibrations of an elastic rod controlled by a distributed force, which is applied to individual sections of the rod, are studied. It is assumed that the force varies in space in a piecewise constant manner. Such a mechanical system can be implemented using piezoactuators attached along the rod. The dynamics of the system is determined from the solution of the variational problem following the method of integrodifferential relations. The variational problem is solved analytically. To do this, traveling waves of the d'Alembert type are introduced on the space-time mesh, which determine continuous displacements and a dynamic potential. The latter relates the momentum density and stresses. A control problem is posed under the condition of the weighted minimization of the vibrational energy stored by the rod at the terminal time instant, and the mean potential energy generated by the control actions. The extremal motion and the corresponding control law are found explicitly by solving the Euler–Lagrange equations. As an example, the control capabilities for certain configurations of piezoelectric elements are studied.

DOI: 10.1134/S1064230723050064

INTRODUCTION

The control problems for systems with distributed parameters arise usually in applications where the description of a mechanical system utilizing one independent variable (for example, time) is not sufficient. Often this leads to the necessity of controlling partial differential equations (PDEs). In this case, the control functions can be included both in the boundary conditions and in the equations themselves [1, 2]. For oscillatory systems, the appearance of control in the boundary conditions means the control by means of of a force, torque, or other quantity given on a part of the boundary (for example, on the edge of a membrane or the end of a rod). This type of actuation seems convenient for engineering applications, but the search for optimal control in this case is difficult, in particular, due to natural limitations on the speed of the control signal [3]. If the control function enters directly into the PDE, then ideally it is possible to control each oscillation mode separately [2, 4], which facilitates the construction of the optimal solution [5]. However, such a distributed control is often difficult to implement directly in applications (for example, due to the need to apply the given force at each point of the membrane/rod). As a consequence, the control function may need to be spatially discretized so that the force acts only on part of the system, or the force is constant over part of the spatial domain.

This paper concerns with a mechanical system in which the control function are discrete and are applied only to certain parts of the object. As a model problem, we study the longitudinal vibrations of a rod, along which length piezoelectric actuators are periodically located. In the intervals between them, control is not applied, and the generated force is considered constant along each actuator, changing only in time and from one actuator to another.

Often, such systems are described by PDEs in which generalized inputs appear on the right-hand sides of the equations due to jumps in forces in space during the transition from the actuator to the load-free section [6]. Thus, the solution can only be constructed in terms of generalized functions. In this paper, the authors use the method of integrodifferential relations (MIDR) [7], which makes it possible to pose a variational problem for system dynamics and find an analytical solution to the optimization problem in the form of continuous functions for continuous initial conditions. A solution is understood as a pair of functions: displacements of the points of the rod and the so-called dynamic potential related by differential relations with momentum and stresses. The dynamics problem is solved using traveling waves of the

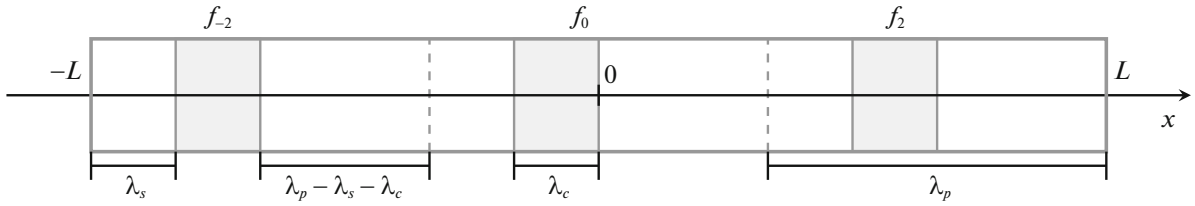

Fig. 1. Diagram of a rod with three control elements.

d'Alembert type, defined on a space-time mesh formed by the characteristics. The optimization problem (weighted minimization of the terminal mechanical energy and energy costs for control) is solved using the Euler–Lagrange equations. In both cases, the unknown variables are found explicitly by resolving the linear relation between the traveling waves and the components of the control vector that arise due to the continuity conditions on the mesh.

Previously, the authors used this approach to construct the optimal control of the longitudinal vibrations of a rod controlled only at the ends, under the terminal conditions while minimizing both the mean mechanical energy [8] and control [9], and also when there are no gaps between distributed control elements. Configurations in which there was no boundary control [10], the general case of using both boundary and distributed control [11], and also the condition of additional control minimization were considered [12]. A particular case of the control horizon, which is a multiple of the dimensionless length of the control element, was studied in [13].

The papers [10, 14] touch upon the issue of the controllability of individual vibrational modes and the separation of modes into groups, each of which is controlled by a certain combination of inputs. The main difference of this article is the presence of gaps between the control elements. For certain configurations, this always leads to the loss of controllability of individual groups of modes, which is an example of uncontrollability of the wave equation when only a part of the length is affected [15]. In addition, the authors show by example that the geometric relationships between the lengths of elements and gaps also determine the efficiency of the control, both in terms of the capability of minimizing mechanical energy and in terms of the energy costs required for the control. The choice of the optimal arrangement of actuators is an extremely important task for engineering applications [16–18], when the relative sizes of the actuators and the controlled system are fixed due to technical limitations. The approach used here can further help in setting and solving similar optimization problems. An example of a study of the control capabilities for various configurations with a fixed minimum size of the actuator relative to the rod length is given.

1. STATEMENT OF THE INITIAL-BOUNDARY VALUE PROBLEM

The longitudinal motions of a thin elastic rod, shown schematically in Fig. 1, are considered. Its length along the x axis is $2L$, the coordinate origin is located in the geometric center of the rod, whose longitudinal stiffness $\kappa > 0$ and linear density $\rho > 0$ do not change along the x axis.

In addition to the elastic force in the cross section of the rod, there is a time-varying $t \geq 0$ controlling force $f(t, x)$, which is piecewise constantly distributed along the length. In a simplified model, such a force can be generated, for example, by groups of piezoelectric actuators (control elements), which create compressive or tensile stresses in individual sections of the rod, highlighted in Fig. 1 in gray for the case of three elements.

In this paper, we restrict ourselves to the periodic arrangement of control elements with the period λ_p, $L = K\lambda_p/2$, $K \in \mathbb{N}$. The length of the only active element on the period is $\lambda_c \leq \lambda_p$. The leftmost element of the rod is spaced at a distance of λ_s from the boundary point with coordinate $x = -L$. Within each control interval $\mathfrak{U}_k = (x_k^-, x_k^+)$ with number $k \in \mathfrak{K}$, the force f is distributed uniformly. Here, for convenience of notation, a set of indices $\mathfrak{K} = \{1 - K, 3 - K, \ldots, K - 1\}$ is introduced with step 2. Outside the control elements, the force f is zero. The coordinates of the ends of the interval $\mathfrak{U}_k$ are defined as

$$x_k^{\pm} = \frac{k-1}{2}\lambda_p + \frac{1 \pm 1}{2}\lambda_c + \lambda_s, \quad k \in \mathfrak{K}.$$

Outside of these control elements, the force f is zero. Thus, the distributed force f is given in the form

$$f(t,x) = \begin{cases} f_k(t), & x \in \mathfrak{U}_k, \quad k \in \mathfrak{K}, \\ 0, & x \in \mathfrak{X} \setminus \bigcup\limits_{k \in \mathfrak{K}} \mathfrak{U}_k. \end{cases} \tag{1.1}$$

As the domain $\mathfrak{D}$ for the variables defining the mechanical state of the rod, we introduce the Cartesian product of the time ($\mathfrak{T}$) and spatial ($\mathfrak{X}$) intervals:

$$\mathfrak{D} = \mathfrak{T} \times \mathfrak{X}, \quad \mathfrak{T} = (0,T), \quad \mathfrak{X} = (-L,L),$$

where T is the control time. For the proposed generalization of the constitutive relations of the system under consideration, the absolute displacements of the rod points $v : \mathfrak{D} \to \mathbb{R}$, the linear momentum density $p : \mathfrak{D} \to \mathbb{R}$, and the total normal force in the cross section $s : \mathfrak{D} \to \mathbb{R}$ are chosen as the unknown variables.

The law of the change of momentum (Newton's second law) connects the two unknown functions p and s:

$$p_t(t,x) = s_x(t,x), \quad (t,x) \in \mathfrak{D}. \tag{1.2}$$

Here subscripts t and x denote the partial derivatives with respect to time and space, respectively. In turn, momentum and force are related to the first derivatives of the displacement function, according to the local constitutive laws:

$$p(t,x) = \rho v_t(t,x), \quad s(t,x) = \kappa v_x(t,x) + f(t,x), \quad (t,x) \in \mathfrak{D}. \tag{1.3}$$

If the function f is differentiable, the classical equation of motion [19] is obtained after substituting (1.3) into (1.2):

$$\rho(x) v_{tt}(t,x) - (\kappa(x) v_x(t,x))_x = f_x, \quad (t,x) \in \mathfrak{D}. \tag{1.4}$$

In terms of the introduced variables, the position and momentum of the rod points are subject to the initial conditions at the time instant $t = 0$:

$$v(0,x) = v^0(x), \quad p(0,x) = p^0(x), \quad x \in \mathfrak{X}, \tag{1.5}$$

where v^0 and p^0 are known sufficiently smooth distributions [20]. The rod ends $x = \pm L$ are unloaded:

$$s(t,-L) = s(t,L) = 0, \quad t \in \mathfrak{T}. \tag{1.6}$$

It should be taken into account that although the function f is piecewise continuous, the rod must remain a solid body, and the force in the section, according to Newton's third law, cannot have jumps. This imposes additional continuity conditions on the functions v and s at the points $x_k^{\pm}$.

According to the MIDRs [7], in order to pass to the generalized formulation of the initial-boundary value problem (1.2)–(1.6), we introduce on the domains $\mathfrak{D}$ a new function (dynamic potential) $r : \mathfrak{D} \to \mathbb{R}$ such that

$$p = r_x, \quad s = r_t. \tag{1.7}$$

By directly substituting (1.7) into (1.2), we verify that Newton's second law is satisfied automatically with such a substitution.

To eliminate variables p and s, it is possible to rewrite the equations of state (1.3) as

$$\begin{cases} r_t(t,x) - \kappa(x) v_x(t,x) = 0, \\ r_x(t,x) - \rho(x) v_t(t,x) = f(t,x), \end{cases} \quad (t,x) \in \mathfrak{D}. \tag{1.8}$$

Both the initial state (1.5) and the boundary conditions (1.6) are expressed via the kinematic and dynamic variables v and r:

$$\begin{gathered} v(0,x) = v^0(x), \quad r(0,x) = r^0(x) = \int\limits_{-L}^{x} p^0(\chi) d\chi + c^0, \quad x \in \overline{\mathfrak{X}}; \\ r(t,L) = r^0(L), \quad r(t,-L) = r^0(-L), \quad t \in \overline{\mathfrak{T}}. \end{gathered} \tag{1.9}$$

We note a feature of such a representation of the mechanical state of the system: the dynamic variable r is specified up to an arbitrary constant c^0, whose value does not affect the motion of the elastic body. The nonzero right parts $r^0(\pm L)$ appear in the boundary conditions specified in (1.9) to ensure the continuity of the solution, as will be shown below. This provides the compatibility of the initial and boundary conditions for $t = 0$ and $x = \pm L$.

2. GENERALIZED FORMULATION OF THE PROBLEM

The local representation of the constitutive laws (1.8) requires a certain smoothness of the initial distribution (1.9) and the applied load f [20]. To consider a wider class of solutions, taking into account the discontinuous nature of the function f, two differential equations (1.8) can be combined, according to the MIDR [7] into one integral relation. Finding a solution in this case is reduced to the conditional minimization of the functional quadratic in the kinematic and dynamic variables v and r.

We formulate the corresponding generalized initial-boundary value problem.

The initial distributions that are square-integrable with their first derivatives $v_0, r_0 \in H^1(\mathfrak{X})$ and the square-integrable force $f \in L^2(\mathfrak{D})$ are given. We find the kinematic and dynamic state functions $v^*(t,x)$ and $r^*(t,x)$ in the space $H^1(\mathfrak{D})$ that minimize the functional

$$\Phi[v^*, r^*] = \min_{vr \in H^1(\mathfrak{D})} \Phi[v,r] = 0, \quad \Phi = \int_{\mathfrak{D}} \varphi d\mathfrak{D} \geq 0, \quad d\mathfrak{D} = dtdx,$$
$$\varphi \triangleq \frac{1}{4}(g^2 + h^2), \quad g \triangleq \sqrt{\rho} v_t - \frac{r_x}{\sqrt{\rho}}, \quad h \triangleq \sqrt{\kappa} v_x - \frac{r_t - f}{\sqrt{\kappa}} \tag{2.1}$$

when the initial and boundary constraints (1.9) are satisfied.

In (2.1) the integral relation $\Phi = 0$, realized on the exact solution, replaces the local constitutive equations (1.8), while the conditional minimization Φ takes place under the strict fulfillment of equalities (1.9). Specially scaled state functions g and h, whose quadratic form φ has the dimension of the linear energy density, are introduced. In turn, the state functional Φ has the dimension of action. The positive value $\Phi[v,r] > 0$ measures the deviation of the approximation (v,r) from the exact solution (v^*, r^*) on which the absolute minimum of the functional is $\Phi = 0$. The requirement of the square integrability of both state functions and their first derivatives in the variational problem (1.9) and (2.1) follows from the fact that Φ includes squares of derivatives with respect to t and x unknown functions v and r.

3. OPTIMAL CONTROL PROBLEM

We introduce the vector function $\mathbf{f} : \mathfrak{T} \to \mathbb{R}^K$, $\mathbf{f} = (f_k)_{k \in \mathfrak{K}}$, whose components are the forces $f_k(t)$ defined in (1.1), created by the kth control element. In terms of $\mathbf{f}$, the following control problem is solved.

We assume, according to (2.1) and taking into account the initial and boundary conditions (1.9), that the functions $v, r \in H^1(\mathfrak{D})$ minimize the state functional Φ for the arbitrary control $\mathbf{f} \in L^2(\mathfrak{T}; \mathbb{R}^K)$, which determines the force f according to (1.1). We find such an admissible vector function $\mathbf{f}^*(t)$ that, on the fixed time interval $\mathfrak{T}$, minimizes the objective functional:

$$\Theta[\mathbf{f}^*] = \min_{\mathbf{f} \in L^2(\mathfrak{T}; \mathbb{R}^K)} \Theta[\mathbf{f}], \quad \Theta = \Upsilon + 10^{\gamma} \Psi,$$
$$\Upsilon = \frac{\lambda_c}{2\kappa T} \int_{\mathfrak{T}} \mathbf{f}^2 dt, \quad \Psi = \int_{\mathfrak{X}} \psi|_{t=T} dx, \quad \psi \triangleq \frac{\kappa v_x^2}{2} + \frac{r_x^2}{2\rho}. \tag{3.1}$$

Problem (3.1) is the problem of finding an extremum under the condition that for an arbitrary vector function $f(t)$ variables v and r provide to the functional Φ from (2.1) the minimum zero values, strictly sutisfying the equality constraints, namely, conditions (1.9). Here Υ is the mean potential energy generated by the force $f(t,x)$, Ψ is the mechanical energy of the rod at the end of the process, $\psi(t,x)$ is the linear energy density, and γ is the dimensionless weighting factor. The solution of the direct problem of dynamics (1.9) and (2.1) is a pair of functions (v,r). The energy density representation ψ includes both variables. The first

term in ψ determines the potential energy of the elastic deformations of the rod in displacements, and the second determines the kinetic energy through the dynamic potential.

To simplify the description of the system, we proceed without loss of generality to dimensionless variables (hereinafter, the index * is omitted):

$$v = Lv^*, \quad r = \kappa\tau_* r^*, \quad x = Lx^*, \quad t = \tau_0 t^*, \quad \tau_*^2 = \frac{L^2\rho}{\kappa}. \tag{3.2}$$

Such a replacement is equivalent to choosing a dynamic system with parameters $L = \rho = \kappa = 1$.

4. SOLUTION OF THE INITIAL-BOUNDARY VALUE PROBLEM

The solution (v, r) to problem (1.9) and (2.1) is sought in the form of traveling waves in the d'Alembert representation. In the general case of an arbitrary set of actuator parameters, the search for an analytical solution is rather difficult. In [10], a particular case of the arrangement of actuators without gaps, i.e., when $\lambda_c = \lambda_p$ and hence $\lambda_s = 0$, was considered. For such a configuration, the system can be reduced in dimensionless time $T \geq 4/K$ into a periodic terminal state with period $\lambda = 2/K$. In terms of eigenfunctions, all modes with wavenumbers that are multiples of $K/2$ are not controllable.

Further, we describe an algorithm for solving the problem for the case in which the length parameters and the control time are multiples of the dimensionless length λ:

$$\begin{gathered} \lambda = 2/N, \quad \lambda_p = N_p\lambda, \quad \lambda_c = N_c\lambda, \quad \lambda_s = N_s\lambda, \quad T = M\lambda, \\ N = KN_p, \quad \{K, M, N_c, N_p\} \subset \mathbb{N}, \quad N_s \in \mathbb{Z}_+, \quad N_c + N_s \leq N_p. \end{gathered} \tag{4.1}$$

The arrangement of control elements is considered periodic when relation (4.1) is satisfied. In other words, counting from the left end of the rod at $x = -1$, first there are $N_s \geq 0$ elementary intervals without actuators each of length λ, then N_c intervals of the same length with actuators. The period can be closed by $N_p - N_c - N_s \geq 0$ intervals again without the actuators. Counting from the right end of the current period, the structure is repeated.

In this proportionate case, it is possible to form a finite mesh of characteristics on the space-time domain $\mathfrak{D}$, on which, as will be shown below, we can exactly solve the initial boundary value problem (1.9) and (2.1). The multiplicity of the number λ of the control time T is not necessary for constructing a finite mesh and obtaining an analytical solution [11], but this leads to more than doubling the number of mesh elements and complicating the solution's algorithm. In this paper, to simplify the presentation, we restrict ourselves to the discrete set of time intervals defined in (4.1).

To build a mesh on the domain $\mathfrak{D}$, we break the time interval $\mathfrak{T}$ into M subintervals $\mathfrak{T}_m$; and the spatial interval $\mathfrak{X}$, into N subintervals $\mathfrak{X}_j$. Thus,

$$\begin{gathered} \mathfrak{T}_m = (t_m, t_{m+1}), \quad t_i = i\lambda, \quad m \in \mathfrak{M} = \{0, \ldots, M-1\}, \\ \mathfrak{X}_j = (x_{j-1}, x_{j+1}), \quad j \in \mathfrak{J} = \{1-N, 3-N, \ldots, N-1\}, \\ x_n = n\lambda/2, \quad n \in \mathfrak{N}^*, \quad \mathfrak{N}^* = \{-N, 2-N, \ldots, N\}. \end{gathered} \tag{4.2}$$

Each interval $\mathfrak{X}_j$ corresponds to an open subdomain $\mathfrak{D}_j = \mathfrak{T} \times \mathfrak{X}_j$ of domain $\mathfrak{D}$ and three one-dimensional functions:

$$\begin{gathered} w_j^+ : (x_{j-1}, T + x_{j+1}) \to \mathbb{R}, \quad w_j^- : (-x_{j+1}, T - x_{j-1}) \to \mathbb{R}, \\ y_j : (0, T) \to \mathbb{R}, \quad y_j(t) = \lambda^{-1} \int\limits_{\mathfrak{X}_j} \int\limits_0^t f(\tau, x) d\tau dx. \end{gathered} \tag{4.3}$$

On the domain $\mathfrak{D}_j$, the desired functions v and r are presented in the form

$$\begin{cases} v(t,x) = w_j^+(t+x) + w_j^-(t-x), \\ r(t,x) = w_j^+(t+x) - w_j^-(t-x) + y_j(t), \end{cases} \quad (t,x) \in \mathfrak{D}_j, \quad j \in \mathfrak{J}. \tag{4.4}$$

Direct substitution shows that the constitutive functional Φ vanishes when relations (4.4) are satisfied, because $r_x = v_t$, $r_t = v_x + f$.

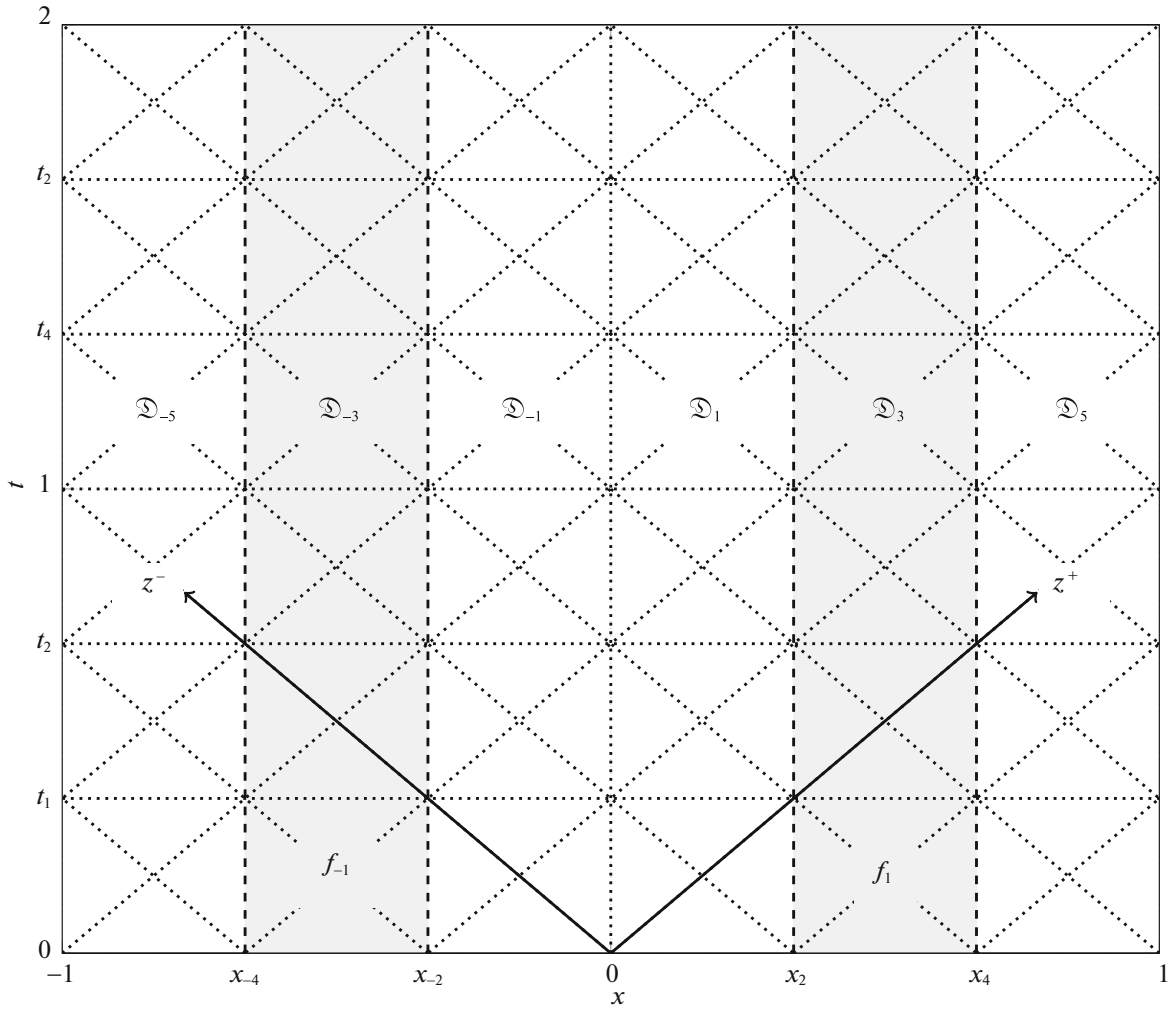

Fig. 2. Grid on the space-time domain $\mathfrak{D}$ for $N = 6$, $K = 2$, $N_c = N_s = 1$, $M = 6$.

We turn to Fig. 2 to see how one-dimensional functions determine solution (4.4) on a two-dimensional domain $\mathfrak{D}$. For compact notation, new coordinates are introduced (z^+, z^-), whose axes are related to two characteristics of the solution (solid oblique lines). The two families of characteristics are the segments in domain $\mathfrak{D}$ on which the values of the functions $w_j^{\pm}(t \pm x)$ do not change. The new coordinates are related to (t, x) by the bijective linear transformations:

$$z^{\pm} = t \pm x, \quad t = \frac{z^+ + z^-}{2}, \quad x = \frac{z^+ - z^-}{2}. \tag{4.5}$$

The oblique mesh edges shown by the dotted line in Fig. 2 are the characteristics defined in the new coordinates as

$$\mathfrak{S}_i^{\pm} = \left\{(z^+, z^-) \in \mathfrak{D} : z^{\pm} = \frac{2i - N}{2}\lambda\right\}, \quad i = 1, \ldots, N + M - 1.$$

The spatial and temporal mesh edges are easier to define in the old coordinates in the form

$$\mathfrak{S}_m^t = \{(t, x) \in \mathfrak{D} : t = t_m\}, \quad t_m = m\lambda, \quad m \in \mathfrak{M}^* = \{0, \ldots, M\};$$
$$\mathfrak{S}_n^x = \{(t, x) \in \mathfrak{D} : x = x_n\}, \quad x_n = \frac{1}{2}n\lambda, \quad n \in \mathfrak{N}^*.$$

To satisfy the continuity conditions on these edges, we need to introduce the following functions on each subdomain $\mathfrak{D}_j$:

$$\begin{gathered} w^{\pm}_{j,m} : \mathfrak{Z} \to \mathbb{R} : \quad w^{\pm}_{j,m}(z) = w^{\pm}_j(z + z^{\pm}_{j,m}), \quad z^{\pm}_{j,m} = z^{\pm}_j + m\lambda, \\ z^{\pm}_j = \frac{\pm j \mp 1}{2}\lambda, \quad j \in \mathfrak{J}, \quad m \in \mathfrak{M}^*, \quad \mathfrak{Z} = (0,\lambda); \\ y_{j,m} : \mathfrak{Z} \to \mathbb{R} : \quad y_{j,m}(z) = y_j(z + t_m), \quad j \in \mathfrak{J}, \quad m \in \mathfrak{M}. \end{gathered} \tag{4.6}$$

According to (4.4), the linear combination of functions $w^+_{i,m}$, $w^-_{j,m}$, and $y_{j,m}$ with a valid index combination i, j, m, and n uniquely defines the state variables v and r on the corresponding triangular mesh element.

Since $v, r \in H^1(\mathfrak{D})$, similar properties follow from the linear dependence for the one-dimensional functions $w^{\pm}_{j,m} \in H^1(\mathfrak{Z})$ and $y_{j,m} \in H^1(\mathfrak{Z})$. By the Sobolev lemma [21], these functions must be continuous and continuously extendable to the closure of their domain: $w^{\pm}_{j,m} \in C^0(\overline{\mathfrak{Z}})$, $y_{j,m} \in C^0(\overline{\mathfrak{Z}})$.

To construct a continuous solution to the initial-boundary value problem on the closure of the domain $\overline{\mathfrak{D}}$, it is necessary to sutisfy the initial, boundary, and interelement conditions on the segments $\mathfrak{S}^t_0$ and $\mathfrak{S}^x_n$, $n \in \mathfrak{N}^*$. Taking into account (1.9), (4.4), (4.6), and the conditions following from (4.3) for the construction $y_{j,0}(0) = 0$, the initial constraints on $\mathfrak{S}^t_0$ for each subdomain $\mathfrak{D}_j$ are presented in the form

$$\begin{cases} w^+_{j,0}(z) + w^-_{j,0}(\lambda - z) = v^0(z + z^+_j), \\ w^+_{j,0}(z) - w^-_{j,0}(\lambda - z) = r^0(z + z^+_j), \end{cases} \quad j \in \mathfrak{J}. \tag{4.7}$$

The boundary conditions from (1.9) for each mesh edge lying on the boundary segments $\mathfrak{S}^x_{\pm N}$ are rewritten in the form

$$\begin{cases} w^+_{N-1,m+1}(z) - w^-_{N-1,m}(z) + y_{N-1,m}(z) = r^0(1), \\ w^+_{1-N,m}(z) - w^-_{1-N,m+1}(z) + y_{1-N,m}(z) = r^0(-1), \end{cases} \quad m \in \mathfrak{M}. \tag{4.8}$$

It is also necessary to add the interelement conditions for the continuity of functions v and r on the inner segments $\mathfrak{S}^x_n$ to these constraints. These conditions are set as follows:

$$\begin{cases} w^+_{n+1,m+1}(z) + w^-_{n+1,m}(z) = w^+_{n-1,m}(z) + w^-_{n-1,m+1}(z), \\ w^+_{n+1,m+1}(z) - w^-_{n+1,m}(z) + y_{n+1,m}(z) = w^+_{n-1,m}(z) - w^-_{n-1,m+1}(z) + y_{n-1,m}(z), \\ m \in \mathfrak{M}, \quad n \in \mathfrak{N} = \{2 - N, 4 - N, \ldots, N - 2\}. \end{cases} \tag{4.9}$$

The number of equations $N_e = 2N(M + 1)$ in the linear algebraic system (4.7)–(4.9) is equal to the number of unknown functions $w^{\pm}_{j,m}$, $j \in \mathfrak{J}$, $m \in \mathfrak{M}^*$. Argument z ranges from 0 to λ. To confirm the solvability of this system with respect to traveling wave functions, we can propose the following algorithm.

First, the initial conditions (4.7) are resolved in pairs: each pair with respect to two variables $w^+_{j,0}$ and $w^-_{j,0}$ for $j \in \mathfrak{J}$. After the appropriate replacement of the argument $z' = \lambda - z$ and constants $z^-_j = z^+_j + \lambda$, the obtained values of these variables are expressed explicitly in terms of the initial distributions:

$$\begin{cases} w^+_{j,0}(z) = \frac{1}{2}v^0(z^+_j + z) + \frac{1}{2}r^0(z^+_j + z), \\ w^-_{j,0}(z') = \frac{1}{2}v^0(z^-_j - z') - \frac{1}{2}r^0(z^-_j - z'), \end{cases} \quad j \in \mathfrak{J}. \tag{4.10}$$

At the second stage, by increasing the index m from 0 to $M - 1$, the boundary and interelement conditions (4.8) and (4.9) are consecutively satisfied. In this case, two boundary equations from (4.8) for the current value of m are allowed relative to variables $w^+_{N-1,m+1}$ and $w^-_{1-N,m+1}$. For the same m equations from (4.9) are solved in pairs $2(N - 1)$ with respect to the functions of traveling waves $w^+_{n+1,m+1}$ and $w^-_{n-1,m+1}$. The functions included in this subsystem with the second index m ($w^{\pm}_{j,m}$, $j \in \mathfrak{J}$) have already been expressed

at the previous steps of the algorithm with respect to the initial functions v^0, r^0, and unknown $y_{j,i}$, $i = 0,\ldots,m-1$, $j \in \Im$.

5. REDUCTION OF THE OPTIMAL CONTROL PROBLEM TO A CLASSICAL VARIATIONAL ONE

Solution to the linear system of equations (4.7)–(4.9) with respect to variables $w^{\pm}_{j,m}$, where $j \in \Im$ and $m \in \mathfrak{M}^*$, depends on the initial distributions $v^0(x)$, $r^0(x)$, $x \in \overline{\mathfrak{X}}$, and functions $y_{j,m}(z)$, $z \in \overline{\mathfrak{Z}}$, with indices $j \in \Im$ and $m \in \mathfrak{M}$. In turn, according to (1.1), (4.3), and (4.6), depending on the location of the interval $\mathfrak{X}_j$ on the x axis, function $y_{j,m}$ is either equal to zero if $\mathfrak{X}_j \subset \mathfrak{X} \backslash \bigcup_{k\in\mathfrak{K}} \mathfrak{U}_k$ or depends on one of the control forces f_k if $\mathfrak{X}_j \subset \mathfrak{U}_k$. To explicitly express this dependence, we introduce new independent control functions:

$$u_{k,m} : \overline{\mathfrak{Z}} \to \mathbb{R} : \quad u_{k,m}(z) = \int_{t_m}^{t_m+z} f_k(\tau)d\tau, \quad k \in \mathfrak{K}, \quad m \in \mathfrak{M}. \tag{5.1}$$

In this representation, $y_{j,m}(z) = u_{k,m}(z)$ provided that $\mathfrak{X}_j \subset \mathfrak{U}_k$. We introduce the control vector function $\mathbf{u} : \overline{\mathfrak{Z}} \to \mathbb{R}^{KM}$ with components

$$\begin{gathered} \mathbf{u} = (u_i)_{i=1}^{KM}, \quad u_j = u_{k,m}, \\ j = M(K-1-k)/2 + m + 1, \quad k \in \mathfrak{K}, \quad m \in \mathfrak{M}. \end{gathered} \tag{5.2}$$

In order for the kinematic and dynamic functions v, r to be continuous, the nodal values of the control functions must be consistent on the segments $\mathfrak{S}^t_m$, $m \in \mathfrak{M}$:

$$u_{k,m}(\lambda) = u_{k,m+1}(0), \quad m \in \mathfrak{M}, \quad u_{k,0}(0) = 0, \quad k \in \mathfrak{K}. \tag{5.3}$$

It is more convenient to represent these ratios in vector form:

$$\mathbf{u}(0) + \mathbf{B}\mathbf{u}(\lambda) = 0, \quad \mathbf{B} \in \mathbb{R}^{(KM)\times(KM)}. \tag{5.4}$$

We consider the structure of the objective functional Θ from (3.1), taking into account the d'Alembert representation and the introduced control functions. Due to its additivity, the functional Υ is rewritten in terms of the control vector function $\mathbf{u}$ as

$$\Upsilon = \frac{\lambda_c}{2\kappa T}\int_0^{\lambda} (\mathbf{u}'(t))^2 dt.$$

Paying attention to the expressions for v and r in (4.4) and taking into account (4.3), the energy density function ψ defined in (3.1) can be represented on the subdomain $\mathfrak{D}_j$:

$$\psi = \psi_j = \frac{1}{2}\Big(w_j^+(t+x) + w_j^+(t-x)\Big)_x^2 + \frac{1}{2}\Big(w_j^+(t+x) - w_j^+(t-x)\Big)_x^2 = \frac{1}{2}(w_j^{+\prime}(z^+))^2 + \frac{1}{2}(w_j^{-\prime}(z^-))^2.$$

Given the coordinate values $z^{\pm}$ at the final time $t = T$, we obtain the expression for the terminal energy of the rod:

$$\Psi = \sum_{j\in\Im}(\Psi_j^+ + \Psi_j^-),$$

$$\Psi_j^{\pm} = \frac{1}{2}\int_{\mathfrak{X}_j} (w_j^{\pm\prime}(T \pm x))^2 dx = \frac{1}{2}\int_0^{\lambda}\left(\frac{d}{dz} w_{j,M}^+(z)\right)^2 dz,$$

$$\Psi = \int_0^{\lambda} \big(\mathbf{A}\mathbf{u}'(z) + \mathbf{a}(z)\big)^2 dz, \quad \mathbf{a} \in \mathbb{R}^{(2N)\times(KM)}, \quad \mathbf{A} : \overline{\mathfrak{Z}} \to \mathbb{R}^{2N}.$$

Here the last line follows from the fact that $2N$ functions $w^+_{j,M}(x)$ as a solution to system (4.7)–(4.9) depend on the initial state and the linear combination of the control functions $u_{k,m}$. This dependence is expressed, respectively, in terms of the given vector function $\mathbf{a}$ and matrix $\mathbf{A}$.

Thus, by presenting the desired v and r as a linear combination of traveling waves that are functions of one variable z, the optimal control problem (1.9)–(3.1) after renormalization is reduced to the classical boundary value problem of the calculus of variations with respect to the first derivative of the vector function $\mathbf{u}(z)$. We need to find the control $\mathbf{u}^*(z)$ on the interval $z \in \overline{\mathfrak{Z}}$ that minimizes the quadratic functional

$$\tilde{\Theta}[\mathbf{u}^*] = \min_{\mathbf{u}\in H^1(\mathfrak{Z};\mathbb{R}^{KM})} \tilde{\Theta}[\mathbf{u}], \quad \tilde{\Theta} = \int_0^\lambda \theta(z, \mathbf{u}'(z))dz,$$
$$\theta = (\mathbf{u}')^2 + \tilde{\gamma}(\mathbf{A}\mathbf{u}' + \mathbf{a})^2, \quad \tilde{\gamma} = 2KT\lambda_c^{-1}10^{\gamma} > 0, \tag{5.5}$$

subject to the boundary conditions (5.4). The square of the vector in (5.5) means the sum of the squares of all its components.

To find the necessary extremality conditions for the solution of the variational problem (5.4) and (5.5), we introduce the vector function adjoint to $\mathbf{u}$, according to

$$\mathbf{p} = \frac{\partial\theta}{\partial\mathbf{u}'} = 2(\mathbf{E} + \tilde{\gamma}\mathbf{A}^{\mathrm{T}}\mathbf{A})\mathbf{u}' + 2\tilde{\gamma}\mathbf{A}^{\mathrm{T}}\mathbf{A}, \tag{5.6}$$

where $\mathbf{E}$ is the identity matrix of the corresponding dimension. Since the Lagrangian θ, introduced in (5.5), includes only the first derivative of $\mathbf{u}$, the Euler equation has the form

$$(\mathbf{E} + \tilde{\gamma}\mathbf{A}^{\mathrm{T}}\mathbf{A})\mathbf{u}''(z) + \tilde{\gamma}\mathbf{A}^{\mathrm{T}}\mathbf{A}'(z) = 0, \quad z \in \mathfrak{Z}. \tag{5.7}$$

We write the problem's transversality condition as

$$\mathbf{p}^{\mathrm{T}}(0)\delta\mathbf{u}(0) - \mathbf{p}^{\mathrm{T}}(\lambda)\delta\mathbf{u}(\lambda) = 0, \tag{5.8}$$

where $\delta\mathbf{u}(0)$ and $\delta\mathbf{u}(\lambda)$ are variations of function $\mathbf{u}$ on the boundary of the domain. Taking into account the essential boundary conditions (5.4), we can derive the natural conditions imposed on the function $\mathbf{p}$ from (5.8):

$$\mathbf{p}(\lambda) = -\mathbf{B}^{\mathrm{T}}\mathbf{p}(0). \tag{5.9}$$

It is important to note that the control vector $\mathbf{u}(t)$, satisfying the necessary stationarity conditions (5.4), (5.7), and (5.9), provides the absolute minimum to the objective functional $\tilde{\Theta}$. This follows directly from the squareness and non-negativity of $\tilde{\Theta}$.

6. ISSUES OF THE CONTROLLABILITY OF THE DYNAMIC SYSTEM

Although the control problem (1.9) and (3.1) does not require a strict translation of the rod to a predetermined state at the end of the process, the value of the minimized mechanical energy Ψ at the instant $t = T$ will directly depend on the resources of the chosen contol structure. Some conclusions about controllability can be drawn using the Fourier method.

We apply the method of the separation of variables for Eq. (1.4) and project it in the space $L^2(\mathfrak{X})$ into the basic functions $\{e_i(x)\}_{i\in\mathbb{Z}_+}$, which are the solution of the corresponding eigenvalue problem

$$e_i''(x) = -\omega_i^2 e_i(x), \quad e_i'(\pm 1) = 0, \quad i \in \mathbb{Z}_+. \tag{6.1}$$

With this approach, the solution to the original initial-boundary value problem can be represented as an expansion in this orthogonal basis in the form

$$v(t,x) = \sum_{i\in\mathbb{Z}_+} e_i(x)v_i(t). \tag{6.2}$$

Using integration by parts and taking into account the discontinuous nature of the force function f from (1.1), we arrive at a linear system of ordinary differential equations:

$$\ddot{v}_i + \omega_i^2 v_i = \sum_{n\in\mathfrak{N}^*} e_i(x_n)y'_n, \quad v_i(0) = v_i^0, \quad \dot{v}_i(0) = p_i^0, \quad i \in \mathbb{Z}_+. \tag{6.3}$$

Here v_i, v_i^0, and p_i^0 are respectively the projections of the solution $v(t,x)$ and initial distributions $v^0(x)$ and $p^0(x)$ on $e_i(x)$. Additionally, in (6.3) the functions of jumps of the integral of force f are introduced:

$$y_n(t) \triangleq y_{n+1}(t) - y_{n-1}(t), \quad n \in \mathfrak{N}^*, \quad y_{-N-1} = y_{N+1} = 0. \tag{6.4}$$

Using the same symbol as for the integral values y_j and for the jumps y_n does not cause contradictions, because the indices of these functions belong to respectively disjoint sets $j \in \mathfrak{J}$ and $n \in \mathfrak{N}^*$ (cf. (4.3)).

Thus, from (6.3) it follows that only the jumps of the integrals affect the motion of the rod. Moreover, the ith mode is uncontrollable if for the arbitrary control $\mathbf{u}$ the right side of the corresponding equation from (6.3) is identically equal to zero:

$$\overline{f}_i(t) \triangleq \sum_{n\in\mathfrak{N}^*} e_i(x_n)y'_n(t) \equiv 0. \tag{6.5}$$

If the values of several eigenfunctions are such that $e_i(x_n) = e_j(x_n)$ at $i \neq j$ for all $n \in \mathfrak{N}^*$, we assume that all these modes belong to the same group. In the case of a homogeneous rod at $\rho = \kappa = 1$ in the dimensionless form, the normalized eigenfunctions have the form

$$\begin{gathered} e_i(x) = \cos\frac{i\pi(x+1)}{2}, \quad \omega_i = \frac{i\pi}{2}, \quad i = 1,2,\ldots, \\ e_0 = \frac{\sqrt{2}}{2}, \quad \omega_0 = 0. \end{gathered} \tag{6.6}$$

The value of the function

$$e_i(x_n) = \cos\frac{i\pi(N+n)}{2N}$$

runs through only a finite number of quantities for each $n \in \mathfrak{N}^*$ at fixed N. Consequently, the number of linear combinations $\overline{f}_i$ introduced in (6.5) is bounded. As a result, all oscillation modes are divided into $N+1$ countable subsystems (groups of modes) with one control input. The group with number $k = 0,\ldots,N$ combines modes with numbers $i = 2Nj \pm k \geq 0$, where $j \in \mathbb{Z}_+$.

Based on the mode expansion (6.3), we come to some a priori ideas about the possibilities of damping oscillations for various configurations of the control elements. As was shown in [10], even in the presence of $K = N$ control elements located without gaps (see the upper left diagram of the rod for $N = 6$ in Fig. 3), we cannot control the zero mode group, i.e., stop the motion of the rod as a whole and change the mode amplitudes with numbers $2iN$, $i \in \mathbb{N}$. Indeed, substituting the values $e_{2jN}(x_n)$, where $j \in \mathbb{Z}_+$, from (6.6) in (6.5) and taking into account (6.4), we obtain

$$\overline{f}_0 = \sqrt{2}(y'_{N+1} - y'_{-N-1})/2 \equiv 0, \quad \overline{f}_{2iN} = y'_{N+1} - y'_{-N-1} \equiv 0, \quad i \in \mathbb{N}.$$

These forces do not depend on the value of other functions y_j, $j \in \mathfrak{J}$; thus, for a fixed number of elementary intervals N for any other control system configurations ($K < N$), the zero mode group remains uncontrollable.

The reduction of the number of the control inputs K can only harm the situation and cause loss of control in other groups. For example, if the control element in each period occupies two elementary intervals ($N_c = 2$, see the third and sixth diagrams from the top on the left in Fig. 3), for the Nth group, the values of the corresponding eigenforms $e_{(2i-1)N}(x_n) = \cos(\pi(N+n)/2)$ at $n \in \mathfrak{N}^*$ and $i \in \mathbb{N}$ at the ends $x = x_k^{\pm}$ of the interval $\mathfrak{U}_k$ are $e_{(2i-1)N}(x_k^+) = e_{(2i-1)N}(x_k^-)$. It directly follows from this that the constant force acting, according to (1.1), on this interval $f(t,x) = f_k(t)$ is included in the linear control combination $\overline{f}_{(2i-1)N}$ of the mode with number $(2i-1)N$ twice with a factor of $+1$ and twice with a factor of -1. Running through all indices $k \in \mathfrak{K}$, we get $\overline{f}_{(2i-1)N}(t) \equiv 0$. This means that modes with numbers iN are uncontrollable for those configurations where $i \in \mathbb{Z}_+$.

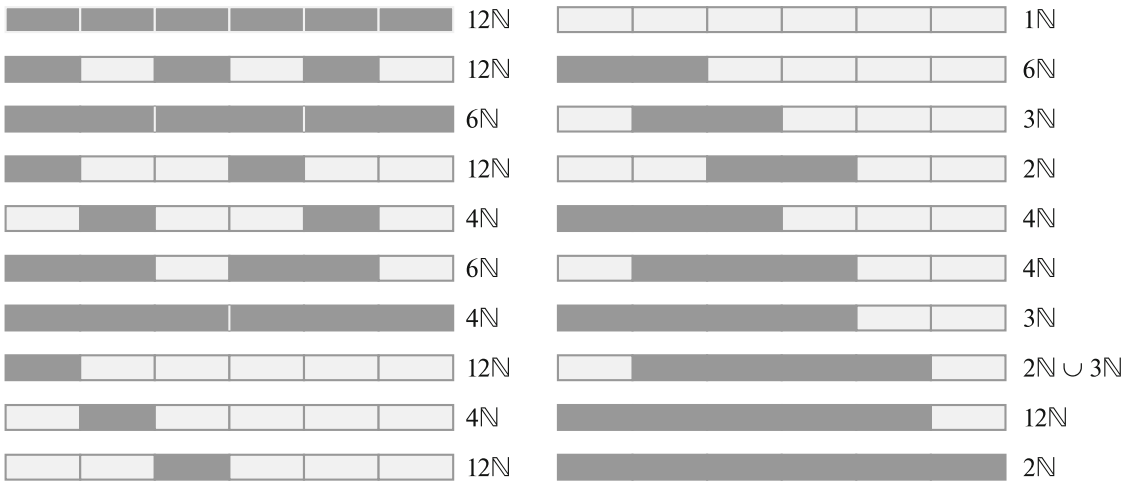

Fig. 3. Possible periodic structures of the rod control at $N = 6$ and the corresponding sets of indices of uncontrolled modes (gray indicates areas with applied forces).

Another interesting example of a structure with additional loss of controllability is the case with a period length of 3λ ($N_p = 3$, $N = 3K$) and $N_s = N_c = 1$ (see, for example, the fifth diagram from the top, on the left in Fig. 3). For this configuration, modes with a wavelength that is a multiple of 3λ (group number $2K$) are uncontrollable. In the considered group of modes, the eigenfunctions e_i take the following values on the boundaries of the intervals $\mathfrak{X}_j$, $j \in \mathfrak{I}$:

$$e_i(x_n) = \cos\left((3K + n)\left(j \pm \frac{1}{3}\right)\pi\right), \quad i = (6j \pm 2)K, \quad j \in \mathbb{Z}_+, \quad n \in \mathfrak{N}^*.$$

At the nodal points $x_k^{\pm}$ of the kth period at the boundary of the control interval $\mathfrak{U}_k$ for $k \in \mathfrak{K}$, the values of the eigenfunctions are the same: $e_i(x_k^+) = e_i(x_k^-)$. Consequently, for these modes, the right-hand sides of Eqs. (6.3) vanish ($\overline{f}_i(t) \equiv 0$).

We can generalize the arguments of the previous paragraph to the case when the control interval $\mathfrak{U}_k$ is located symmetrically on the kth period of the structure, i.e., when $N_p = 2N_s + N_c$. Taking into account the symmetry with respect to the center of the period of the eigenfunctions e_i with a long wavelength multiple $N_p\lambda$, it can be argued that the linear combination $\overline{f}_i$ of the control force function f_k will include N_i times both with the coefficient $+c$ and with the coefficient $-c$. This leads to the uncontrollability of the ith mode.

7. AN EXAMPLE OF MOTION OPTIMIZATION

For clarity, we consider an example of the optimal control of the longitudinal displacements of an elastic rod for the given time $T = 3$. The following parameters of the structure of control elements are selected: $K = 3$, $N = 6$, $N_c = 1$, and $N_s = 0$ ($N_p = 2$, $M = 9$). This means that three periods fit along the length of the rod, each of which is divided into two identical sections: on the left with control; and on the right, without control (see the diagram second from the top on the left in Fig. 3). The initial conditions are taken as

$$v^0(x) = -r^0(x) = a\cos\frac{4\pi x}{3}, \quad a^2 = \frac{9}{\pi(16\pi - 3\sqrt{3})}. \tag{7.1}$$

Coefficient a is chosen so that the initial mechanical energy of the system is equal to 1. Despite that the trigonometric function in the initial conditions are even, the momentum density function $p^0(x)$ is antisymmetric with respect to the origin, since, according to (1.9), it is equal to the derivative r_x^0, which is odd in coordinate x. From (7.1) it follows that the center of mass of the rod is at rest at the time instant $t = 0$. For the system under consideration, the center of mass in the absence of external forces will remain motionless over the entire time interval $t \in [0, T]$.

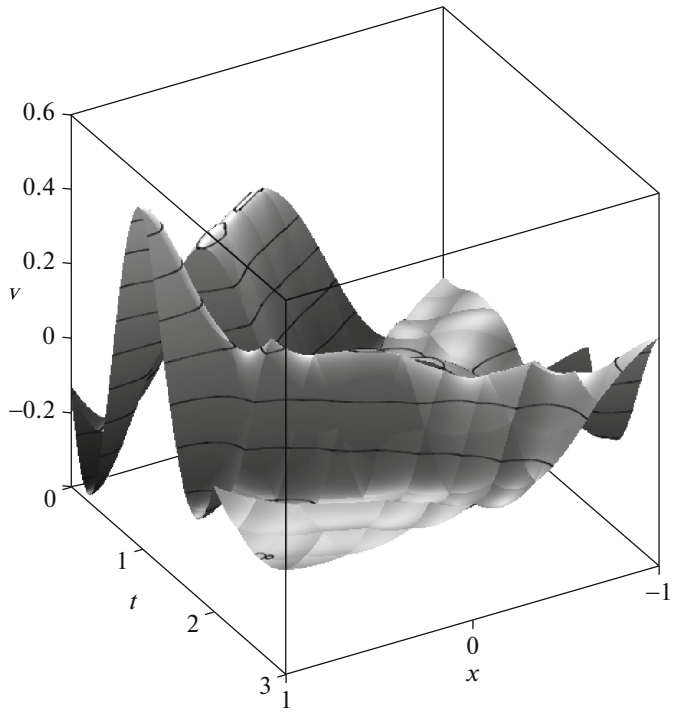

Fig. 4. Optimal rod displacements $v(t, x)$ at $\gamma = -1$.

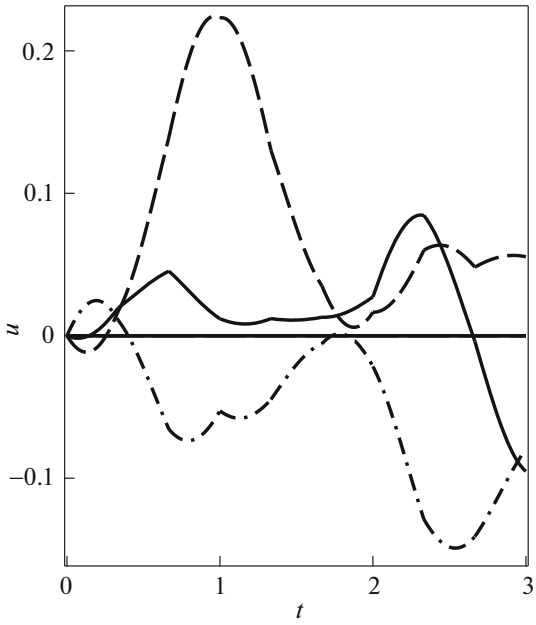

Fig. 5. Optimal control inputs $u_k(t)$ at $\gamma = -1$ for $k = -2$ (solid line), $k = 0$ (dashed line), and $k = 2$ (dashed-dotted line).

For the weighting factor $\gamma = -1$, the optimal displacements of the rod points $v(t, x)$ is shown in Fig. 4. When choosing such a parameter, more attention is paid to reduce the intensity of the control (the square of the norm $\Upsilon = 0.01794$), which leads to sufficiently large residual deformations (terminal energy $\Psi = 0.08846$). As can be seen from the plot, the displacement function is continuous, but breaks are visible, located on the characteristics shown in Fig. 2 by the dashed lines for other system parameters.

The optimal control integrals $u_k(t)$, which act on the rod within the intervals $\mathfrak{U}_k = \mathfrak{X}_j$, where $k = -2, 0, 2$ and $j = -5, -1, 3$, are shown in Fig. 5 as solid, dashed, and dashed-dotted lines, respectively.

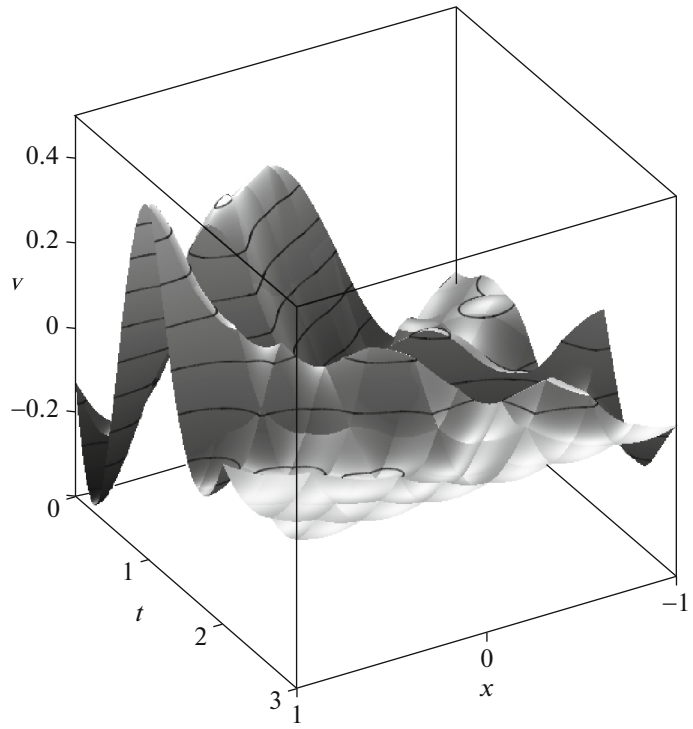

Fig. 6. Optimal rod displacements $v(t, x)$ at $\gamma = 1$.

These are continuous functions with the initial values equal to zero by construction. For the chosen initial conditions (7.1), the control integrals are linear combinations of trigonometric and polynomial functions.

We choose the weight coefficient equal to $\gamma = 1$. In this case, to minimize the input signals, a larger control resource is required ($\Upsilon = 0.03957$), while the residual energy decreases by more than 2 orders of magnitude ($\Psi = 0.00831$) compared to the initial one. The corresponding optimal displacements are shown in Fig. 6. As can be seen, although the terminal deformations have decreased, there are still uncontrolled vibrational modes with a period that is a multiple of $\lambda = 1/3$. In Fig. 7, almost doubling of the amplitude of the force integrals $u_k(t)$ can be seen (cf. Fig. 5).

The dependence of the optimal values of the mean square of the control vector Υ on the time parameter M and weighting factor γ are shown on a logarithmic scale in Fig. 8. Υ reaches its highest values at $M = 3$ and large positive values γ. With a further increase in time T in the same range of values γ, the control functional Υ decreases monotonically.

The terminal energy of rod Ψ shown in Fig. 9, also depending on γ and M, decreases monotonically with increasing time. At $M \geq 4$ and positive values of γ, this functional rapidly approaches the limiting value $\Psi^* = 0.00829$, equal to the total energy of modes with numbers $i \in 12\mathbb{N}$ (see Section 6). In a short period of time T or for negative values of γ, the energy barely changes during the control process and remains close to 1.

8. ANALYSIS OF THE OPTIMAL VALUES OF OBJECTIVE FUNCTIONALS

We study the behavior of the optimal values of the squared control norm Υ and the terminal mechanical energy Ψ defined in (3.1) when changing the configuration of the piezoelectric elements (Table 1). For example, we take the initial conditions (7.1), fix the number of elementary intervals $N = 6$, time parameter $M = 12$ ($T = 4$), and weighting factor $\gamma = 3$. Sufficiently large values of M and γ are chosen in order to achieve extremely low energies Ψ at the point in time T. As the calculations show, the further increase either M or γ does not lead to a noticeable decrease in the terminal energy.

Up to symmetry about the origin of coordinates $x = 0$, all possible periodic locations and sizes of control elements, indicated on each diagram with a gray background, are shown for the chosen parameter N

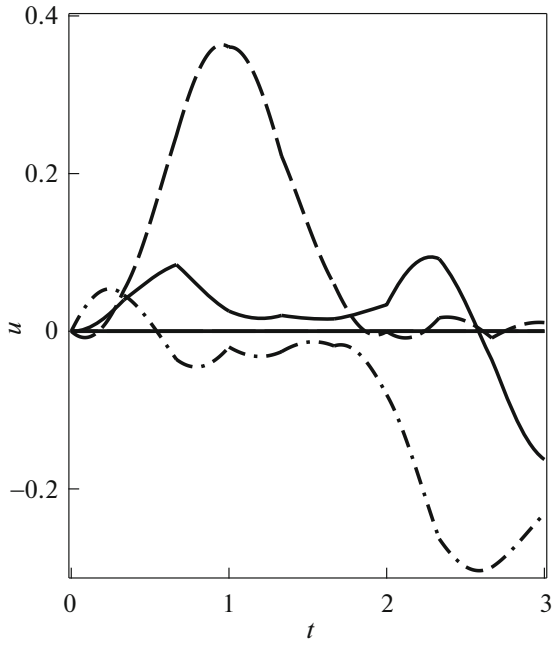

Fig. 7. Optimal control inputs $u_k(t)$ at $\gamma = 1$ for $k = -2$ (solid line), $k = 0$ (dashed line), and $k = 2$ (dashed-dotted line).

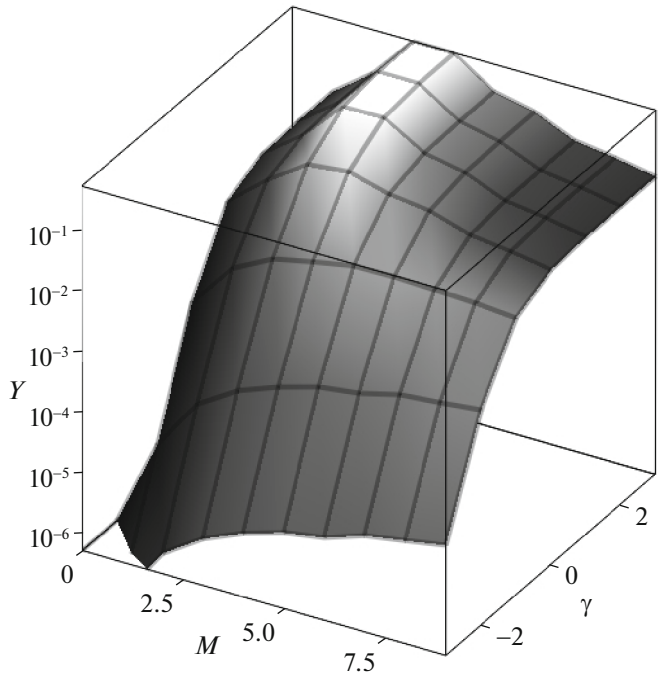

Fig. 8. The dependence of the optimal value of functional Υ on the time parameter M and weighting factor γ.

in Fig. 3. To the right of the diagram, the corresponding set of mode numbers is symbolically indicated, to which no control actions are applied for the given configuration.

The first basic scheme on the left in Fig. 3 corresponds to the case with the maximum number of control inputs, $K = N = N_p = N_c = 6$. It includes the first six numbers in the second row from the top in the table. Due to the greater control resource, at the end of the process, it is possible to reach a state with a rather low energy $\Psi = \Psi^* \approx 0.008$ at the lowest control norm $\sqrt{\Upsilon}$. In this case, every twelfth oscillation mode, counting from zero, is uncontrollable.

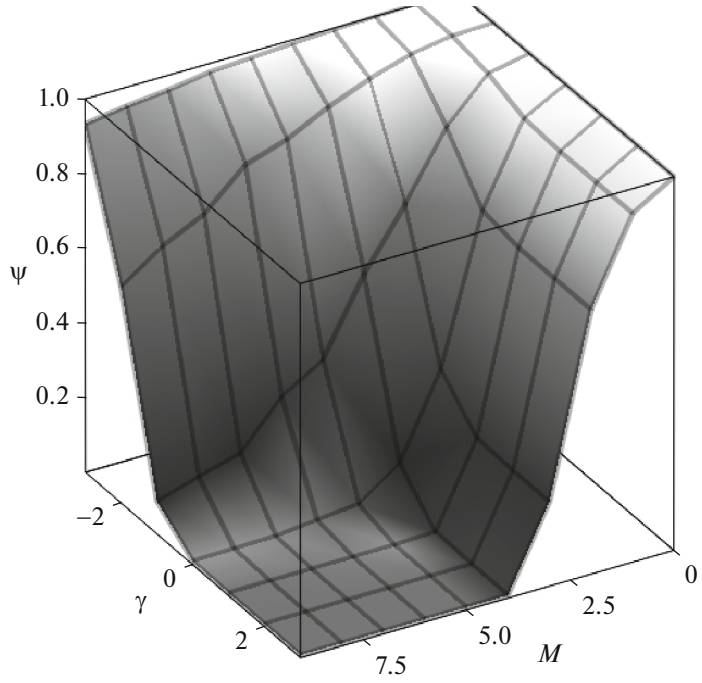

Fig. 9. The dependence of the optimal value of functional Ψ on the time parameter M and weighting factor γ.

The same efficiency in suppressing vibrations can be achieved by using three control inputs of a short length ($K = 3$, $N_c = 1$, see the second diagram on the top left in Fig. 3). However, this results in a more intensive control: the functional Υ doubles (third row of the table, left half). It should be noted that for this scheme, the critical time to reach the minimum energy value is doubled with $T^* = 2/3$ for $K = 6$ to $T^* = 4/3$; see [10]. For the same dimension $K = 3$ of the control vector $\mathbf{u}(t)$, increasing the length of the control element up to $|\mathfrak{U}_k| = 2/3$ ($N_c = 2$, the third scheme from the top in Fig. 3 on the left and the fourth row in the left half of the table) leads to a loss of controllability of every sixth mode and to a noticeable increase in the residual vibrations.

The next four diagrams in Fig. 3 on the left (fourth to seventh from the top) show the possible locations and lengths of the controls for the case $K = 2$ and $N_p = 3$. At $N_c = 1$ and $N_s = 0$, it is again possible to reach the minimum energy value $\Psi = \Psi^*$, although the control functional Υ increases by more than four

Table 1. Optimal values of functionals Υ and Ψ for various configurations of control elements with $M = 2N = 12$ and $\gamma = 10^3$

N_p	N_c	N_s	Υ	Ψ	N_p	N_c	N_s	Υ	Ψ
1	1	0	0.01033	0.00829	0	0	0	0	1
2	1	0	0.02066	0.00829	6	2	0	0.04274	0.04205
2	2	0	0.01434	0.04205	6	2	1	0.02243	0.49284
3	1	0	0.04266	0.00829	6	2	2	0.01349	0.5
3	1	1	0.02256	0.16823	6	3	0	0.07285	0.16823
3	2	0	0.02197	0.04205	6	3	1	0.10309	0.16823
3	3	0	0.03643	0.16823	6	4	0	0.03756	0.49284
6	1	0	0.17171	0.00829	6	4	1	0.00273	0.95079
6	1	1	0.04512	0.16823	6	5	0	0.42874	0.00829
6	1	2	0.07994	0.00829	6	6	0	0.03125	0.5

times compared to the basic case at $N_p = N_c = 1$. The shortest time required to reach this energy also increases up to $T^* = 2$. It is interesting to note the scheme with two control elements at $N_c = N_s = 1$ (fifth row in Fig. 3). The terminal energy Ψ increases by a factor of more than 20 times with this symmetrical arrangement of the control element in the period. It can be shown that modes with numbers divisible by 4 become uncontrollable for such a scheme. For the dual input configurations with $N_c = 2$ or $N_c = 3$, the oscillation amplitudes of either every fourth or every sixth mode, respectively, cannot be changed.

The rest of the diagrams in Fig. 3 (except the first one on the top right, without actuators) correspond to the case of one control signal $K = 1$, otherwise $N_p = 6$. Among them, we would like to highlight three configurations with parameters $N_c = 1$ and $N_s = 0$; $N_c = 1$ and $N_s = 2$; and $N_c = 5$ and $N_s = 0$. For them for the time $T \geq T^* = 3$ we can achieve the lowest level of residual energy for all the considered schemes $\Psi = \Psi^*$. Of the first two configurations with a short control element $N_c = 1$, the second option with a larger shift of the element to the center of the rod turns out to be more advantageous in terms of control costs. The most disadvantageous of the three configurations is the configuration with a long element, $N_c = 5$.

For the case with one control signal, it is worth noting two schemes with a symmetrical arrangement of the element relative to the geometric center: these are the configurations with parameters $N_c = N_s = 2$ and $N_c = 6$ ($N_s = 0$). Due to the aforementioned symmetry, all even modes turn out to be uncontrollable, and for the initial conditions (7.1), they contain exactly half of the energy stored by the rod (see the left half of the table, the fifth row from the top and the last row). For the same initial conditions, the largest vibrations remain for the symmetric case $N_c = 4$ and $N_s = 1$, when it is not possible to control not only the even modes but also the modes with the indices divisible by 3.

The selected examples of the arrangement of control elements, due to their limitations, do not allow us to draw unambiguous conclusions about the possibilities of the structural optimization of the investigated dynamic system with distributed parameters. At the same time, it should be pointed out that a reasonable reduction in the size of the piezoelectric elements in violation of both the geometric symmetry of their arrangement and the proportionality of various parts of the configuration can have a positive affect on increasing the control efficiency in terms of reducing the rate of the input signals and the energy of the residual oscillations.

CONCLUSIONS

The longitudinal displacements of a thin homogeneous elastic rod with a periodic structure of piezoelectric elements are considered. A generalized formulation of the initial-boundary value problem, whose solution is sought with respect to the kinematic and dynamic variables in the energy space, is given. For the case of a rod controlled by longitudinal forces discretely distributed in space, with the given control law, an algorithm for constructing the optimal motion in the form of a combination of traveling waves is proposed. For a fixed control time interval, a solution is found to the problem of minimizing the objective functional, which is the weighted sum of the squared norm of the control vector and the terminal mechanical energy of the rod. For this, a two-dimensional control problem in space and time is reduced to a one-dimensional variational problem with fixed ends. The dependence of the optimal values of the norm of the integral of the piezoelectric force and the terminal energy on the control time and the weight coefficient is studied. The change in these values for a number of configurations of the control elements is demonstrated. The proposed approach makes it possible to compare the effectiveness of different control structures and thus to pose in a certain sense the problem of finding the optimal configuration.

FUNDING

This work was supported by the Russian Science Foundation, project no. 21-11-00151.

CONFLICT OF INTEREST

The authors declare that they have no conflicts of interest.

REFERENCES

1. J. L. Lions, *Optimal Control of Systems Governed by Partial Differential Equations* (Springer, New York, 1971).

2. A. G. Butkovskii, *Theory of Optimal Control of Systems with Distributed Parameters* (Nauka, Moscow, 1965) [in Russian].

3. I. V. Romanov and A. S. Shamaev, On a boundary controllability problem for a system governed by the two-dimensional wave equation, J. Comput. Syst. Sci. Int. **58** (1), 105–112 (2019).

4. F. L. Chernous'ko, I. M. Anan'evskii, and S. A. Reshmin, *Control Methods for Nonlinear Mechanical Systems* (Fizmatlit, Moscow, 2006) [in Russian].

5. G. Chen, "Control and stabilization for the wave equation in a bounded domain. II," SIAM J. Control Optim. **19** (1), 114–122 (1981).

6. I. Kucuk, I. Sadek, and Y. Yilmaz, "Optimal control of a distributed parameter system with applications to beam vibrations using piezoelectric actuators," J. Franklin Inst. **351** (2), 656–666 (2014).

7. G. V. Kostin and V. V. Saurin, *Dynamics of Solid Structures. Methods Using Integrodifferential Relations* (De Gruyter, Berlin, 2018).

8. A. A. Gavrikov and G. V. Kostin, "Optimal control of longitudinal motion of an elastic rod using boundary forces," J. Comput. Syst. Sci. Int. **60** (5), 740–755 (2021).

9. G. Kostin and A. Gavrikov, "Energy-optimal control by boundary forces for longitudinal vibrations of an elastic rod," in *Lecture Notes in Mechanical Engineering: Proceedings of the XLIX International Summer School-Conference "Advanced Problems in Mechanics", 2021, St. Petersburg, Russia* (Springer, 2023).

10. G. Kostin and A. Gavrikov, "Controllability and optimal control design for an elastic rod actuated by piezoelements," IFAC-PapersOnLine **55** (16), 350–355 (2022).
https://doi.org/10.1016/j.ifacol.2022.09.049

11. G. Kostin and A. Gavrikov, "Optimal motions of an elastic structure under finite-dimensional distributed control," 2023. https://arxiv.org/pdf/2304.05765.
https://doi.org/10.48550/arXiv.2304.05765.

12. G. Kostin and A. Gavrikov, "Optimal Motion of an Elastic Rod Controlled by Piezoelectric Actuators and Boundary Forces," in *16th Int. Conf. "Stability and Oscillations of Nonlinear Control Systems" (Pyatnitskii Conference) (STAB)* (IEEE, Moscow, 2022), pp. 1–4.
https://doi.org/10.1109/STAB54858.2022.9807484.

13. G. Kostin and A. Gavrikov, "Modeling and optimal control of longitudinal motions for an elastic rod with distributed forces," 2022. https://arxiv.org/pdf/2206.06139.
https://doi.org/10.48550/arXiv.2206.06139.

14. A. Gavrikov and G. Kostin, "Optimal LQR control for longitudinal vibrations of an elastic rod actuated by distributed and boundary forces," in *Mechanisms and Machine Science* (Springer, Berlin, 2023), **Vol. 125**, pp. 285–295.
https://doi.org/10.1007/978-3-031-15758-5_28

15. L. F. Ho, "Exact controllability of the one-dimensional wave equation with locally distributed control," SIAM J Control Optim. **28** (3), 733–748 (1990).

16. I. Bruant, G. Coffignal, F. Lene, and M. Verge, "A Methodology for determination of piezoelectric actuator and sensor location on beam structures," J. Sound Vib. **243** (5), 861–882 (2001).
https://doi.org/10.1006/jsvi.2000.3448

17. V. Gupta, M. Sharma, and N. Thakur, "Optimization criteria for optimal placement of piezoelectric sensors and actuators on a smart structure: A technical review," J. Intell. Mat. Syst. Struct. **21** (12), 1227–1243 (2010).
https://doi.org/10.1177/1045389X10381659

18. F. Botta, A. Rossi, and N. P. Belfiore, "A novel method to fully suppress single and bimodal excitations due to the support vibration by means of piezoelectric actuators," J. Sound Vib. **510** (13), 116260 (2021).
https://doi.org/10.1016/j.jsv.2021.116260

19. A. N. Tikhonov and A. A. Samarskii, *Equations of Mathematical Physics* (Nauka, Moscow, 1977) [in Russian].

20. S. G. Mikhlin, *Course of Mathematical Physics* (Nauka, Moscow, 1968) [in Russian].

21. K. Yosida, *Functional Analysis* (Springer, Berlin, 1968; Mir, Moscow, 1968).